HHS Public Access

Author manuscript

Cancer Res. Author manuscript; available in PMC 2017 May 15.

Published in final edited form as:

Cancer Res. 2016 May 15; 76(10): 3045–3056. doi:10.1158/0008-5472.CAN-15-2310.

Extracellular adenosine production by ecto-5′-nucleotidase (CD73) enhances radiation-induced lung fibrosis

Florian Wirsdörfer[1,*], **Simone de Leve**[1,*], **Federica Cappuccini**[1,*,§], **Therese Eldh**[2], **Alina V. Meyer**[1], **Eva Gau**[1], **Linda F. Thompson**[3], **Ning-Yuan Chen**[4], **Harry Karmouty-Quintana**[4], **Ute Fischer**[5], **Michael Kasper**[6], **Diana Klein**[1], **Jerry W. Ritchey**[7], **Michael R. Blackburn**[4], **Astrid M. Westendorf**[8], **Martin Stuschke**[9], and **Verena Jendrossek**[1,#]

[1]Institute of Cell Biology (Cancer Research), University of Duisburg-Essen, Medical School, Virchowstrasse 173, Essen, Germany

[2]Department of Radiation Oncology, University Hospital Tübingen, Hoppe-Seyler-Straβe 3, Tübingen, Germany

[3]Immunobiology and Cancer Program, Oklahoma Medical Research Foundation, 825 N.E. 13th Street, Oklahoma City, Oklahoma, USA

[4]Department of Biochemistry and Molecular Biology, University of Texas - Health Science Center, 6431 Fannin Suite 6.200, Houston, Texas, USA

[5]Department of Pediatric Oncology, Hematology and Clinical Immunology, University Children's Clinic, Medical Faculty, Heinrich-Heine-University, Moorenstr. 5, Düsseldorf, Germany

[6]Institute of Anatomy, Medical Faculty Carl Custav Carus, Technische Universität Dresden, Dresden, Germany

[7]Department of Veterinary Pathobiology, Center for Veterinary Health Sciences, Oklahoma State University, Stillwater Oklahoma, USA

[8]Department of Infection Immunology, Institute of Medical Microbiology, Medical Faculty, University of Duisburg-Essen, Essen, Germany

[9]Department of Radiation Oncology, University Hospital Essen, Hufelandstrasse 55, Essen, Germany

Abstract

Radiation-induced pulmonary fibrosis is a severe side effect of thoracic irradiation, but its pathogenesis remains poorly understood and no effective treatment is available. In this study, we investigated the role of the extracellular adenosine as generated by the ecto-5'-nucleotidase CD73 in fibrosis development after thoracic irradiation. Exposure of wild-type C57BL/6 mice to a single

[#]Correspondence to: Dr. Verena Jendrossek, Institute of Cell Biology (Cancer Research), Department of Molecular Cell Biology, University of Duisburg-Essen, Medical Faculty, Virchowstrasse 173, 45122 Essen, Germany, FAX: +49-201-723 5904; Phone: +49-201-723 3380; verena.jendrossek@uni-due.de.

[*]equal contribution

[§]current address: ORCRB, The Jenner Institute, University of Oxford, Oxford, UK

Conflict of interest notification:

No conflict of interest does exist for any of the authors

dose (15 Gray) of whole thorax irradiation triggered a progressive increase in CD73 activity in the lung between 3 and 30 weeks post-irradiation. In parallel, adenosine levels in bronchoalveolar lavage fluid (BALF) were increased by approximately three-fold. Histological evidence of lung fibrosis was observed by 25 weeks after irradiation. Conversely, CD73-deficient mice failed to accumulate adenosine in BALF and exhibited significantly less radiation-induced lung fibrosis ($P<0.010$). Furthermore, treatment of wild-type mice with pegylated adenosine deaminase (PEG-ADA) or CD73 antibodies also significantly reduced radiation-induced lung fibrosis. Taken together, our findings demonstrate that CD73 potentiates radiation-induced lung fibrosis, suggesting that existing pharmacological strategies for modulating adenosine may be effective in limiting lung toxicities associated with the treatment of thoracic malignancies.

Keywords

ionizing radiation; fibrosis; CD73; adenosine; normal tissue toxicity

Introduction

Radiotherapy is an integral part of standard treatment for thorax-associated neoplasms. Unfortunately, adverse late effects in the highly radiosensitive lung limit the radiation dose resulting in suboptimal local control, metastases and decreased quality of life (1, 2). Lung toxicity also limits the dose of total body irradiation in conditioning regimens for hematopoietic stem cell transplantation (3). Acute damage to resident cells induced by thorax irradiation triggers complex reciprocal interactions between damaged resident lung cells, recruited immune cells, extracellular matrix molecules, secreted cytokines/chemokines, growth factors, and proteases resulting in a disturbed balance between inflammatory and repair processes, tissue disorganization, pathologic remodeling and lung fibrosis (2, 4, 5). As a consequence, pneumonitis and pulmonary fibrosis develop within 12 weeks and 6–24 months after radiotherapy, respectively, in patients and mice with symptoms including nonproductive cough, dyspnea, and respiratory insufficiency and a lethality rate up to 10% (1–3, 6). As no available therapies completely prevent or treat these potentially life-threatening adverse late effects, there is a great need for a better understanding of the underlying mechanisms (7, 8).

Ecto-5′-nucleotidase (NT5E, CD73) and adenosine play critical roles in balancing tissue inflammation and repair processes in pulmonary fibrosis, regulating leukocyte extravasation and function, and modulating epithelial cell behavior, vascular function, and cell death (9–16). Herein, CD73 is found on the surface of various cell types in the lung. It acts in concert with ectonucleoside triphosphate diphosphohydrolase 1 (ENTPD1, CD39) to generate adenosine from extracellularly released ATP/ADP. Extracellular adenosine levels are usually low due to rapid cellular uptake by nucleoside transporters and catabolic conversion by adenosine deaminase (ADA) or adenosine kinase to inosine or AMP, respectively. However, they can rapidly increase in response to stress or tissue injury through either direct release from damaged cells or ATP/ADP catabolism by CD39 and CD73 (9, 10). Extracellular adenosine acts through four different G protein-coupled adenosine receptors (ADORA1, ADORA2A, ADORA2B, ADORA3) that are widely expressed and have various biological

functions aimed at maintaining or restoring tissue homeostasis (9, 10, 17). Though CD73 and adenosine are crucial for the regulation of lung homeostasis, their role during radiation-induced pneumopathy is unknown. As earlier reports showed both tissue-protective and pro-fibrotic effects of CD73 and adenosine in pulmonary fibrosis (18–20), we asked whether they would be protective or harmful in radiation-induced lung disease and evaluated their potential as therapeutic targets.

Methods

Mice

C57BL/6 wild-type (WT; Charles River, Sulzfeld, Germany) and CD73$^{-/-}$ (*Nt5e*$^{-/-}$) mice on the C57BL/6 background (12) were bred and housed under specific pathogen-free conditions in Laboratory Animal Facilities of the University Hospitals Tübingen and Essen. Experimental protocols were approved by the appropriate Animal Protection Boards.

In vivo treatment

Eight-to-twelve week old mice were anesthetized with 2% isoflurane, placed in holders and irradiated either with a single dose of 0 (sham control) or 15 Gray (Gy) over their right hemithorax, using a linear accelerator (4.7 Gy/min), or over their whole thorax (WTI) using a Cobalt-60 source (Phillips, Hamburg, Germany; 0.5 Gy/min) as described previously (21, 22).

Some WT mice were exposed to WTI and subsequently treated twice weekly from week 16 to week 25 or 26 post-irradiation by intraperitoneal injection with 100 μl PBS (solvent), 5 Units of pegylated ADA (PEG-ADA) to catabolize adenosine (23), or 100 μg of anti-CD73 mAb TY/23 to inhibit CD73 function (24).

Mice were sacrificed at 3, 6, 12, 16, 20, 24, or 25–30 weeks post-irradiation and blood serum, lung tissue, and/or bronchoalveolar lavage fluid (BALF) were collected.

CD73 enzyme assay

CD73 ecto-5′-nucleotidase enzyme activity was evaluated in frozen lung tissue by measuring the proportion of [^{14}C]IMP converted to [^{14}C]inosine that could be inhibited by the specific CD73 inhibitor adenosine 5′-(α,β-methylene)diphosphate (APCP, Sigma-Aldrich, Munich, Germany) as described previously (12, 25). CD73 activity was expressed as μmol IMP hydrolyzed/h/mg protein.

Determination of albumin in BALF

Albumin levels in BALF were determined using the Albumin ELISA Quantification Kit Mouse (Bethyl Laboratories, Montgomery, USA) according to manufacturer’s instructions (26).

Quantification of apoptosis in BALF

Active caspase-3 in BALF was detected using Caspase-Glo 3/7 Kit (Promega, Mannheim, Germany) as described previously (26).

Nucleotide and nucleoside quantification

AMP and adenosine were measured in BALF by reverse-phase HPLC as previously described (27). For this, lungs were lavaged 4× with 0.3 ml of PBS with 10 μM dipyridamole, 10 μM APCP and 10 μM adenosine deaminase inhibitor 2'-deoxycoformycin (Sigma-Aldrich, Munich, Germany) to prevent adenosine degradation.

Histopathology

Paraffin-embedded tissue—Lungs were isolated from euthanized mice after intratracheal perfusion with 4% paraformaldehyde in PBS (pH 7.2) and fixed overnight in the same solution. Upon dehydration, lungs were embedded in paraffin and sectioned into 5 μm slices.

Frozen tissue—Lungs of euthanized mice were inflated with a 1:1 mixture of Tissue-Tek® O.C.T.™ Compound (Sakura Finetek, Staufen, Germany) and PBS, isolated and placed in O.C.T. embedding medium, pre-cooled on dry ice, and stored at −80°C. Frozen tissue was cut into 7 μm cryosections.

Caspase 3—Immunohistochemical staining of paraffin-embedded lung tissue was performed as described before (26) using an active caspase-3 antibody (New England Biolabs, Frankfurt am Main, Germany), anti-rabbit IgG, Streptavidin AP Complex ready to use, and Fast red staining (Roche, Penzberg, Germany).

Osteopontin (SPP1, OPN), Collagen Type 1 (COL1A1, Col1a1)—Tissue slides were deparaffinised, rehydrated and steam boiled in citrate buffer pH 6. After blocking endogenous peroxidase with 3% H_2O_2, sections were blocked for 20 min with 2% fetal calf serum (osteopontin) or 2% normal goat serum (collagen) and subsequently incubated with anti-osteopontin (R&D Systems, Wiesbaden, Germany) or anti-collagen type 1 antibodies (Rockland Inc., Pottstown, USA) overnight at 4°C. Primary antibodies were detected by secondary antibodies linked to horseradish peroxidase and subsequent DAB staining.

TGF-β (TGFB1), α-SMA (ACTA2)—Immunohistochemical staining of paraffin-embedded lung tissue slides was performed using the Mouse on Mouse (M.O.M.™) ImmPRESS™ HRP (Peroxidase) Polymer Kit (Vector Laboratories, Burlingame, USA) according to the manufacturer's instructions. Anti-transforming growth factor beta (TGF-β) (R&D Systems, Wiesbaden, Germany) and anti-smooth muscle actin (α-SMA) (Merck Millipore, Darmstadt, Germany) were used as mouse primary antibodies. ImmPACT™ VIP Peroxidase (HRP) Substrate Kit (Vector Laboratories) was used to detect TGF-β and α-SMA according to the manufacturer's instructions. Stained sections were counterstained with hematoxylin.

Fibrosis—Lung sections were stained with hematoxylin and eosin (H&E) or Masson´s Goldner Trichrome (MT) (Carl Roth Karlsruhe, Germany), and scored by three individuals blinded to the genotype and treatment group. Ten random, non-overlapping fields (magnification, ×200) of lung parenchyma from each specimen were photographed and lung

fibrosis was scored using a 0 to 8 point *Ashcroft* scale (28). The mean scores for each observer were averaged to yield the final score for each specimen.

CD73 histochemistry—CD73 ecto-5'-nucleotidase enzyme activity was visualized on tissue sections by histochemistry as previously described (29). For a negative control, 5'-AMP was replaced by non-hydrolyzable 5'-AMP. In other experiments the CD73 inhibitor APCP (Sigma Aldrich, Munich, Germany) was added.

Quantitative real-time PCR

RNA was isolated using RNeasy Mini Kit (74106, Qiagen, Hilden, Germany) according to the manufacturer's instructions. Expression levels were normalized to the reference gene (β-actin; set as 1). Quantitative real-time PCR (qPCR) was carried out using specific oligonucleotide primers (β-Actin (*Actb*): fw, CCAGAGCAAGAGAGGTATCC; rev, CTGTGGTGGTGAAGCTGTAG; Fibronectin (*Fn1*): fw, GAAACCTGCTTCAGTGTGTCTG; rev, TTGAATTGCCACCATAAGTCTG; Osteopontin (*Spp1*): fw, ATCTCCTTGCGCCACAGAAT; rev, CTGCCCTTTCCGTTGTTGTC; TGF−β −1 (*Tgfb1*): fw, ACCTGGGTTGGAAGTGGAT; rev, GAAGCGCCCGGGTTGTGTTGGTT) using qPCR MasterMix for SYBR® Assay ROX (SN2X-03T, Eurogentec, Cologne, Germany) according to the manufacturer's instructions.

Lung leukocyte phenotyping

Lung cells were isolated as described previously (22) and stained with anti-CD45 PacificBlue (30-F11), anti-CD11c APC (N418), anti-CD4 APC (RM4–5), anti-CD8 PE (53–6.7), anti-FoxP3 (FJK-16s) and/or anti-CD73 PECy7 (TY/11.8). Antibodies were obtained from BD Biosciences (Heidelberg, Germany), BioLegend (Fell, Germany) or eBioscience (Frankfurt, Germany). Flow cytometry was performed on a LSRII flow cytometer using FACS DIVA software (BD Bioscience, Heidelberg, Germany) and FlowJo (Tree Star, Ashland, USA).

Statistics

Statistical analyses were performed using Prism 5.0 (GraphPad, La Jolla, USA). For normalization, sham control values were set to 100% and values for irradiated animals were displayed as % of sham controls. Student's two-tailed unpaired t tests were used to compare differences between two groups. One-way ANOVA followed by Newman-Keuls multiple comparison tests were used to compare more than two groups. Two-way ANOVA with post-hoc Bonferroni's multiple comparison tests were used to compare groups split on two independent variables. Statistical significance was set at $P<0.05$.

Results

Thorax irradiation triggers up-regulation of CD73, progressive adenosine accumulation in the lung, and pulmonary fibrosis

To gain insight into the role of CD73 in radiation-induced pneumopathy we first examined the effects of a single high dose (15 Gy) WTI on CD73 expression in lungs of WT C57BL/6 mice. We used a histochemical CD73 assay in which the release inorganic phosphate from

the exogenously added substrate 5′-AMP is converted into an insoluble black lead sulfide precipitate. CD73 activity was barely detectable in lungs of control mice at all time points (Fig. 1A). In contrast, we observed a time-dependent increase in lead sulfide precipitation indicative of enhanced AMPase-activity in the lung tissue of mice exposed to WTI (Fig. 1A). There was no non-specific nucleotidase activity as evidenced by a lack of 3′-AMP hydrolysis (Fig. 1A, right panels).

Next we examined whether up-regulation of CD73 expression was associated with increased generation of adenosine by comparing time-dependent changes in lung CD73 enzymatic activity and adenosine levels in the BALF of mice exposed to 0 or 15 Gy WTI. Irradiated mice displayed a time-dependent progressive increase in lung CD73 enzyme activity compared to sham controls culminating in a 3.7-fold rise by 25–30 weeks; no significant differences were seen in control mice (Fig. 1B). WTI also led to time-dependent adenosine accumulation in the BALF, suggesting that radiation-induced up-regulation of CD73 triggers enhanced generation of adenosine. This started at 16 weeks post-irradiation and persisted until the end of the observation time (Fig. 1C).

There was no significant increase in AMPase activity that was not inhibited by the CD73 inhibitor APCP, suggesting that CD73 is the main AMPase contributing to increased adenosine production after WTI (data not shown).

Although the first signs of matrix deposition were detectable at 20 weeks (but not at 16 weeks) post-irradiation, histological signs of lung fibrosis became clearly visible in irradiated WT mice only at 24 to 30 weeks (Fig. 1D). These findings demonstrate that CD73 activity increases prior to the development of lung fibrosis.

WTI led to an increase in the percentage of $CD73^+$ lung cells and the level of CD73/cell compared to sham controls; Fig. 2A depicts a representative histogram of whole lung cells isolated 6 weeks post-irradiation. We observed an increase in $CD45^+$ leukocytes in the lungs of WT mice at 12–24 weeks post-irradiation that was paralleled by a gradual increase in cells with CD73 surface expression reaching a maximum at weeks 25–30 post-irradiation (Fig. 2B, D). Instead, $CD45^-$ cells showed a temporary increase in the proportion of $CD73^+$ cells at week 12 post-irradiation that was however associated with a transient drop in their number in lung tissue during this intermediate phase (Fig. 2C, E).

The above data suggested a contribution of $CD45^+$ cells in radiation-induced CD73 up-regulation. We next evaluated the specific roles of $CD4^+$ and $CD8^+$ lymphocytes and alveolar macrophages, as these are major immune cells infiltrating the irradiated lung (22). While the percentages of $CD73^+CD4^+$ T cells were increased at most time points (Fig. 2F), the percentages of $CD73^+CD8^+$ T cells did not change (Fig. 2G). In contrast, the percentages of $CD73^+$ alveolar macrophages were transiently increased at 6 and 12 weeks post-irradiation (Fig. 2H). Notably, we found largely increased percentages of $CD4^+FoxP3^+$ regulatory T cells (Tregs) during the pneumonitic (early) and fibrotic (late) phases (Fig. 2I). Tregs generally express CD73 (14) (Fig. 2J), and may thus be a major source of adenosine production from $CD45^+$ cells during the fibrotic phase.

Genetic deficiency of CD73 partially protects from early radiation-induced injury

Early damage to resident cells is thought to be linked to fibrosis development (2, 4, 26). For example, fibrosis-prone C57BL/6 mice develop a transient disturbance of blood air barrier function and increased apoptosis of bronchial epithelial cells 3 weeks after hemithorax irradiation (26). To determine whether CD73 influences these early pathophysiologic alterations associated with radiation-induced lung disease, we compared albumin levels in the BALF of WT and $CD73^{-/-}$ mice 3 weeks post-irradiation. Albumin-leakage into the BALF was significantly reduced in $CD73^{-/-}$ mice compared to WT mice (Fig 3A), indicating that loss of CD73 provides partial protection from radiation-induced barrier dysfunction.

WTI also triggered a significant increase in active caspases in the BALF of WT and $CD73^{-/-}$ mice after 3 weeks, but the absolute levels of caspase-activation were again significantly lower in knockout mice (Fig. 3B). Consistent with these findings more bronchial epithelial cells expressed high levels of active caspase-3 in tissue sections of irradiated WT than $CD73^{-/-}$ mice (Fig. 3C). The higher sensitivity of $CD73^{+/+}$ bronchial epithelial cells to radiation-induced apoptosis may contribute to the more pronounced barrier function disturbance observed in WT mice.

In contrast, there were no significant differences in the percentages of $CD45^{+}$ cells in the lungs of WT and $CD73^{-/-}$ mice after WTI (Fig. 3D). These data demonstrate that loss of CD73 partially protects mice from radiation-induced early damage to resident cells without influencing radiation-induced leukocyte recruitment.

$CD73^{-/-}$ mice show reduced adenosine levels and lung fibrosis after WTI

To determine whether CD73 is required for radiation-induced adenosine accumulation, we compared radiation-induced changes in the relative levels of adenosine and its precursor AMP in $CD73^{+/+}$ and $CD73^{-/-}$ mice. As our initial data indicated pronounced CD73 activity at the time of fibrosis development, we performed these investigations 30 weeks after irradiation. WT mice accumulated high levels of BALF adenosine at this time point whereas AMP levels were low (Fig. 4A); in contrast, irradiated $CD73^{-/-}$ mice had low levels of BALF adenosine but high levels of AMP (Fig. 4B). These findings strongly suggest that the elevated adenosine levels in lungs of irradiated WT mice result indeed from CD73-mediated enzymatic conversion of AMP to adenosine.

To examine the role of CD73 in radiation-induced lung fibrosis, we next compared histological changes in WT and $CD73^{-/-}$ mice 30 weeks after WTI using hematoxylin and eosin (H&E)- and MT-stained lung sections (Fig. 4C, D). We observed slightly increased thickening of alveolar septa in non-irradiated $CD73^{-/-}$ mice perhaps due to higher levels of basal tissue inflammation; however, there was little collagen deposition visible in non-irradiated WT or $CD73^{-/-}$ mice (Fig. 4D left panels). Importantly, lung sections from irradiated WT mice revealed a prominent thickening of alveolar septa, increased collagen deposition, and multiple fibrotic foci, well-known fibrosis-associated lung lesions (28); in contrast, lung sections of irradiated $CD73^{-/-}$ mice displayed fewer and less severe lesions yielding a significantly lower Ashcroft score (Fig. 4C, D).

To corroborate our findings we quantified the fibrosis-associated proteins fibronectin, collagen Type 1 (Col1a1) and α-SMA during the fibrotic phase. While WTI triggered a significant increase in fibronectin mRNA expression in WT mice, it enhanced fibronectin-expression in $CD73^{-/-}$ mice to a lesser degree (Fig. 4E). Similarly, a significant accumulation of Col1a1 and α-SMA protein occurred only in lungs of irradiated WT mice, particularly in fibrotic areas. In contrast, only low levels of Col1a1 were detected in the lung sections of irradiated $CD73^{-/-}$ mice and α-SMA expression was hardly detectable except for vascular structures (Fig. 4F, G).

To strengthen the above observations we additionally analyzed the expression of the pro-fibrotic cytokines osteopontin (OPN) and TGF-β, known to be associated with fibrosis development in patients (30, 31). WTI induced higher levels of OPN and TGF-β in paraffin-embedded tissue sections of WT mice compared to $CD73^{-/-}$ mice at ≥ 25 weeks post-irradiation, particularly in the fibrotic areas (Fig. 5A, B). These findings were confirmed by qPCR analysis of their expression levels in whole lung tissue (Fig. 5C, D).

Taken together, the inability of $CD73^{-/-}$ mice to accumulate adenosine in response to WTI correlates with a significant reduction in the expression of fibrosis-associated proteins and a significant attenuation of radiation-induced lung fibrosis. In line with these observations $CD73^{-/-}$ mice also showed improved survival after irradiation (88% vs. 76% for WT mice) and improved health as shown by normal weight gain. In contrast, WT mice exposed to WTI displayed a significantly reduced weight gain at 30 weeks post-irradiation (108±6.5%) compared to 135%±18% for non-irradiated controls.

Targeting adenosine accumulation or CD73 attenuates radiation-induced lung fibrosis

To confirm the involvement of adenosine and CD73 in the pathogenesis of radiation-induced lung fibrosis, we treated WT mice with either PEG-ADA, to catabolize adenosine (23) or with CD73 mAb TY/23 that has proven activity for therapeutic inhibition of CD73 function in mice (32). Based on the kinetics of CD73 increase and adenosine accumulation (Fig. 1B, C), treatment was initiated 16 weeks after WTI (Fig. 6A). PEG-ADA significantly reduced BALF adenosine levels and almost completely abrogated the radiation-induced increase in lung CD73 activity (Fig. 6B, C). Even more important, PEG-ADA reduced the severity of radiation-induced lung fibrosis (represented by the Ashcroft Score) in all treated mice by almost 40% ($P< 0.01$) (Fig. 6D, E) and also significantly reduced fibronectin expression (Fig. 6F). Similarly, TY/23 significantly reduced lung CD73 activity (Fig. 6C). Although TY/23 did not significantly decrease BALF adenosine levels (data not shown), it significantly reduced fibronectin expression and severity of radiation-induced lung fibrosis in all treated mice by more than 25% ($P<0.05$) (Fig. 6D, E). These findings suggest that local concentrations of adenosine in the vicinity of relevant adenosine receptors may have been decreased. The above observations demonstrate that therapies aimed at reducing local adenosine concentrations in lung tissue through increasing its catabolism or through targeting CD73 can protect the lung from the adverse effects of thorax irradiation.

Discussion

Here we demonstrate for the first time that CD73-generated adenosine plays a crucial role in the pathogenesis of radiation-induced lung fibrosis, a dose-limiting side effect of thorax irradiation, and show that CD73 and adenosine are new targets for therapeutic intervention. Thoracic irradiation triggered up-regulation of CD73 in lung tissue, progressive accumulation of adenosine in the BALF, increased expression of pro-fibrotic mediators such as OPN and TGF-β, and lung fibrosis. $CD73^{-/-}$ mice were protected from early damage to resident lung cells, the progressive increase of BALF adenosine, the accumulation of OPN and TGF-β, and exhibited attenuated lung fibrosis. Importantly, treatment with a CD73 antibody or inhibition of adenosine accumulation with PEG-ADA beginning at 16 weeks post-irradiation significantly reduced the severity of radiation-induced fibrosis. We hypothesize that up-regulation of CD73 in response to thoracic irradiation leads to a sustained increase in pulmonary adenosine promoting pathologic tissue remodeling and progression of chronic lung inflammation to fibrosis.

Our findings corroborate earlier reports of reduced liver and skin fibrosis in $CD73^{-/-}$ mice induced by CCl_4 and thioacetamide or bleomycin, respectively (33, 34). In contrast, acute bleomycin-induced pulmonary fibrosis was exacerbated in $CD73^{-/-}$ mice (18). Later work revealed that inhibition of the low affinity ADORA2B attenuates bleomycin-induced pulmonary fibrosis in chronic disease models (19, 35). Thus, the beneficial or disease-promoting effects of adenosine vary depending on the tissue, the type of injury and acute vs. chronic disease stages and may be dictated by the local expression of specific adenosine receptors (19, 36, 37).

Lung injury induced by ionizing radiation resulted in delayed acute inflammation after 3–6 weeks that developed into chronic inflammation and progressed to fibrosis after 25–30 weeks (6, 21). Chronic inflammation was associated with a constant increase in $CD73^{+}CD45^{+}$ leukocytes in the lung as of 12 weeks and an accumulation of $CD73^{+}CD4^{+}$ T cells including $CD4^{+}FoxP3^{+}$ Tregs, during the fibrotic phase. We therefore postulate that thorax irradiation induces a chronic disease state where the tissue-destructive and pro-fibrotic effects of adenosine prevail so that abrogation of CD73 activity or adenosine accumulation has a net benefit.

Convincing evidence that chronically elevated adenosine causes pulmonary injury and fibrosis comes from studies of ADA-deficient mice; these have markedly elevated adenosine levels and die from respiratory distress caused by lung inflammation and progressive airway remodeling (23, 38). Thus, the increased CD73 activity and pulmonary adenosine levels in irradiated WT mice likely amplify pro-fibrotic signaling. In other published studies, adenosine promoted progression of skin, liver and peritoneal fibrosis, mainly via the ADORA2A (36, 39), and fibrotic lung disease mainly by activation of the ADORA2B (35, 40).

Interestingly, thorax irradiation triggered up-regulation of OPN during the fibrotic phase in WT mice, but not in $CD73^{-/-}$ mice, suggesting that the CD73/adenosine axis is a major inducer of OPN in irradiated lung tissue. OPN is also elevated in alveolar macrophages of

ADA-deficient mice by activation of the ADORA2B suggesting that adenosine and OPN contribute to the pathogenesis of the COPD-like syndrome in these mice (40). OPN is produced by diverse resident and immune cells and is associated with fibroblast-activation, wound healing, inflammation and fibrosis in multiple organs, including lung fibrosis induced by bleomycin (41–43). Importantly, it constitutes a valid serum biomarker of lung fibrosis in idiopathic pulmonary fibrosis patients (30). Therefore, we speculate that radiation-induced accumulation of adenosine may promote fibrosis by amplifying pro-fibrotic signaling through induction of OPN and that OPN may represent a biomarker for adverse late effects after lung irradiation.

$OPN^{-/-}$ mice show reduced expression of pro-fibrotic TGF-β, particularly in macrophages, and reduced TGF-β-dependent fibroblast activation (43). Therefore, the reduced TGF-β levels observed in irradiated $CD73^{-/-}$ mice may result from a missing adenosine/OPN-amplification loop. However, TGF-β levels were not altered in $OPN^{-/-}$ $ADA^{-/-}$ mice suggesting that high adenosine levels are sufficient to induce TGF-β expression (40). Tregs may also contribute to TGF-β accumulation under pathological conditions (44). As TGF-β induces Tregs and CD73 expression (45), the accumulation of $CD73^{+}CD4^{+}FoxP3^{+}$ Tregs in fibrotic lungs of irradiated mice could be caused by pathologic adenosine accumulation, high TGF-β levels, or both, and subsequently contribute to additional TGF-β secretion and CD73-dependent adenosine generation (14, 44). We therefore hypothesize that adenosine-induced accumulation of TGF-β and Tregs provides a feed-forward mechanism for progressive accumulation of adenosine and TGF-β. Consistent with this concept, preliminary data indicate that irradiated $CD73^{-/-}$ mice do not accumulate Tregs during the fibrotic phase (unpublished observations).

As ADA-deficient mice can be rescued by enzyme replacement therapy with PEG-ADA to decrease tissue adenosine levels (38), we tried PEG-ADA as well as targeting CD73 with mAb TY/23 to treat irradiated mice. Both treatments significantly reduced radiation-induced lung fibrosis. Although TY/23 did not decrease adenosine accumulation in the BALF as much as PEG-ADA, it was nearly as effective in reducing radiation-induced lung fibrosis. TY/23 may impact local adenosine receptor signaling, yet not cause a measurable decrease in BALF adenosine levels. It is not surprising that PEG-ADA is more effective at reducing BALF adenosine levels, as it should degrade all extracellular adenosine including that generated by CD73-independent mechanisms such as release from cells damaged during lavage.

Surprisingly, CD73 loss also reduced the damaging effects of thorax irradiation on resident lung cells and the blood-air barrier at 3 weeks, a time when increased numbers of $CD73^{+}CD45^{-}$ resident cells and $CD73^{+}CD45^{+}CD4^{+}$ T cells are observed in WT mice. As the magnitude of radiation-induced early damage to resident lung cells correlates with adverse late effects (2, 4) these findings suggest that $CD73^{-/-}$ mice are protected from lung fibrosis in part due to attenuation of CD73-dependent early damage to resident cells. We therefore postulate that the benefit of radiotherapy may be further improved when CD73 inhibition is initiated at earlier time points.

Despite the obvious benefits of CD73 deficiency after WTI, targeting of CD73 or adenosine with TY/23 or PEG-ADA did not provide complete protection. The beneficial effects of adenosine in other models of lung inflammation and fibrosis make it highly likely that therapeutic inhibition of CD73 may blunt protective effects of CD73-dependent adenosine signaling that limit radiation-induced tissue damage and the resulting inflammation particularly during acute disease stages. For example, ADORA2A signaling via CD73-generated adenosine may suppress inflammatory functions of the innate and adaptive immune systems, modulate angiogenesis and matrix-induced pro-inflammatory and pro-fibrotic signaling, and induce Tregs which are known to contribute to adenosine-mediated resolution of acute lung injury (17, 46). Intriguingly, we observed pulmonary accumulation of $CD73^{+}CD4^{+}FoxP3^{+}$ Tregs during the pneumonitic and fibrotic phases upon WTI. However, the specific roles played by Tregs, additional CD73-expressing immune cells, resident endothelial and epithelial cells or fibroblasts and specific adenosine receptors in radiation-induced fibrosis remain to be explored.

Certainly, the tissue-, injury- and disease stage-dependent beneficial or adverse effects of adenosine demand further investigation to define the optimal therapeutic target and treatment schedule. Moreover, any pharmacologic strategies targeting the CD73/adenosine pathway for protection against radiation-induced fibrosis will require careful testing as they may bring complications such as excessive inflammation or autoimmunity by abrogating protective signals mediated by various adenosine receptors, particularly during acute disease stages (47–50). Nevertheless, therapeutic inhibition of CD73 activity or adenosine accumulation provided a significant protection of mice against radiation-induced lung fibrosis offering new opportunities for therapeutic intervention.

In tumor-bearing mice, CD73 and adenosine promote tumor immune escape (51, 52). Intriguingly, radio(chemo)therapy triggers up-regulation of CD73 and CD39 in circulating immune cells of cancer patients and may thereby dampen anti-tumor immune responses (53). It is therefore likely that pharmacologic modulation of the CD73/adenosine pathway may provide a clear therapeutic gain in cancer treatment through multiple mechanisms including immune enhancement (10, 32) and protection of normal tissues against the adverse effects of radio(chemo)therapy by abrogating pro-fibrotic adenosine signals.

Multiple approaches for pharmacologic modulation of adenosine levels exist and some (TY/23, APCP, PEG-ADA) have already been used successfully in preclinical models (17, 32, 54) and PEG-ADA has been given to ADA-deficient patients for decades. Thus, there is every reason for optimism that targeting the CD73/adenosine pathway offers new strategies to limit lung toxicity during therapeutic whole-body or thorax irradiation.

Acknowledgments

We thank Gabriele von Kürthy, Michael Groneberg, Fayong Luo and Stephanie McGee for excellent technical support.

Supported by grants of the Doctoral Programs of the Deutsche Forschungsgemeinschaft (DFG) grant numbers GRK1739/1 and JE275/4-1 (V. Jendrossek), the Bundesministerium für Bildung und Forschung (BMBF) grant number 02NUK024D (V. Jendrossek), and the NIH grant AI18220 (L. F. Thompson).

References

1. Ding NH, Li JJ, Sun LQ. Molecular mechanisms and treatment of radiation-induced lung fibrosis. Current drug targets. 2013; 14:1347–1356. [PubMed: 23909719]
2. Graves PR, Siddiqui F, Anscher MS, Movsas B. Radiation pulmonary toxicity: from mechanisms to management. Semin Radiat Oncol. 2010; 20:201–207. [PubMed: 20685583]
3. Kelsey CR, Horwitz ME, Chino JP, Craciunescu O, Steffey B, Folz RJ, et al. Severe pulmonary toxicity after myeloablative conditioning using total body irradiation: an assessment of risk factors. International journal of radiation oncology, biology, physics. 2011; 81:812–818.
4. Kasper M, Haroske G. Alterations in the alveolar epithelium after injury leading to pulmonary fibrosis. Histol Histopathol. 1996; 11:463–483. [PubMed: 8861769]
5. Tsoutsou PG, Koukourakis MI. Radiation pneumonitis and fibrosis: mechanisms underlying its pathogenesis and implications for future research. International journal of radiation oncology, biology, physics. 2006; 66:1281–1293.
6. Heinzelmann F, Jendrossek V, Lauber K, Nowak K, Eldh T, Boras R, et al. Irradiation-induced pneumonitis mediated by the CD95/CD95-ligand system. J Natl Cancer Inst. 2006; 98:1248–1251. [PubMed: 16954477]
7. Koukourakis MI. Radiation damage and radioprotectants: new concepts in the era of molecular medicine. The British journal of radiology. 2012; 85:313–330. [PubMed: 22294702]
8. Bentzen SM. Preventing or reducing late side effects of radiation therapy: radiobiology meets molecular pathology. Nature reviews Cancer. 2006; 6:702–713. [PubMed: 16929324]
9. Eltzschig HK, Sitkovsky MV, Robson SC. Purinergic signaling during inflammation. The New England journal of medicine. 2012; 367:2322–2333. [PubMed: 23234515]
10. Antonioli L, Blandizzi C, Pacher P, Hasko G. Immunity, inflammation and cancer: a leading role for adenosine. Nature reviews Cancer. 2013; 13:842–857. [PubMed: 24226193]
11. Linden J. Regulation of leukocyte function by adenosine receptors. Adv Pharmacol. 2011; 61:95–114. [PubMed: 21586357]
12. Thompson LF, Eltzschig HK, Ibla JC, Van De Wiele CJ, Resta R, Morote-Garcia JC, et al. Crucial role for ecto-5'-nucleotidase (CD73) in vascular leakage during hypoxia. J Exp Med. 2004; 200:1395–1405. [PubMed: 15583013]
13. Thompson LF, Takedachi M, Ebisuno Y, Tanaka T, Miyasaka M, Mills JH, et al. Regulation of leukocyte migration across endothelial barriers by ECTO-5'-nucleotidase-generated adenosine. Nucleosides, nucleotides & nucleic acids. 2008; 27:755–760.
14. Deaglio S, Dwyer KM, Gao W, Friedman D, Usheva A, Erat A, et al. Adenosine generation catalyzed by CD39 and CD73 expressed on regulatory T cells mediates immune suppression. J Exp Med. 2007; 204:1257–1265. [PubMed: 17502665]
15. Kaku H, Cheng KF, Al-Abed Y, Rothstein TL. A novel mechanism of B cell-mediated immune suppression through CD73 expression and adenosine production. J Immunol. 2014; 193:5904–5913. [PubMed: 25392527]
16. Mikhailov A, Sokolovskaya A, Yegutkin GG, Amdahl H, West A, Yagita H, et al. CD73 participates in cellular multiresistance program and protects against TRAIL-induced apoptosis. J Immunol. 2008; 181:464–475. [PubMed: 18566412]
17. Hasko G, Linden J, Cronstein B, Pacher P. Adenosine receptors: therapeutic aspects for inflammatory and immune diseases. Nature reviews Drug discovery. 2008; 7:759–770. [PubMed: 18758473]
18. Volmer JB, Thompson LF, Blackburn MR. Ecto-5'-nucleotidase (CD73)-mediated adenosine production is tissue protective in a model of bleomycin-induced lung injury. J Immunol. 2006; 176:4449–4458. [PubMed: 16547283]
19. Zhou Y, Schneider DJ, Morschl E, Song L, Pedroza M, Karmouty-Quintana H, et al. Distinct roles for the A2B adenosine receptor in acute and chronic stages of bleomycin-induced lung injury. J Immunol. 2011; 186:1097–1106. [PubMed: 21149612]
20. Chunn JL, Molina JG, Mi T, Xia Y, Kellems RE, Blackburn MR. Adenosine-dependent pulmonary fibrosis in adenosine deaminase-deficient mice. J Immunol. 2005; 175:1937–1946. [PubMed: 16034138]

21. Eldh T, Heinzelmann F, Velalakan A, Budach W, Belka C, Jendrossek V. Radiation-induced changes in breathing frequency and lung histology of C57BL/6J mice are time- and dose-dependent. Strahlentherapie und Onkologie : Organ der Deutschen Rontgengesellschaft [et al]. 2012; 188:274–281.
22. Wirsdorfer F, Cappuccini F, Niazman M, de Leve S, Westendorf AM, Ludemann L, et al. Thorax irradiation triggers a local and systemic accumulation of immunosuppressive CD4+ FoxP3+ regulatory T cells. Radiat Oncol. 2014; 9:98. [PubMed: 24766907]
23. Blackburn MR, Aldrich M, Volmer JB, Chen W, Zhong H, Kelly S, et al. The use of enzyme therapy to regulate the metabolic and phenotypic consequences of adenosine deaminase deficiency in mice Differential impact on pulmonary and immunologic abnormalities. The Journal of biological chemistry. 2000; 275:32114–32121. [PubMed: 10908569]
24. Yamashita Y, Hooker SW, Jiang H, Laurent AB, Resta R, Khare K, et al. CD73 expression and fyn-dependent signaling on murine lymphocytes. European journal of immunology. 1998; 28:2981–2990. [PubMed: 9808167]
25. Thompson LF, Boss GR, Spiegelberg HL, Jansen IV, O'Connor RD, Waldmann TA, et al. Ecto-5'-nucleotidase activity in T and B lymphocytes from normal subjects and patients with congenital X-linked agammaglobulinemia. J Immunol. 1979; 123:2475–2478. [PubMed: 315423]
26. Cappuccini F, Eldh T, Bruder D, Gereke M, Jastrow H, Schulze-Osthoff K, et al. New insights into the molecular pathology of radiation-induced pneumopathy. Radiotherapy and oncology : journal of the European Society for Therapeutic Radiology and Oncology. 2011; 101:86–92. [PubMed: 21722981]
27. Wakamiya M, Blackburn MR, Jurecic R, McArthur MJ, Geske RS, Cartwright J Jr, et al. Disruption of the adenosine deaminase gene causes hepatocellular impairment and perinatal lethality in mice. Proceedings of the National Academy of Sciences of the United States of America. 1995; 92:3673–3677. [PubMed: 7731963]
28. Ashcroft T, Simpson JM, Timbrell V. Simple method of estimating severity of pulmonary fibrosis on a numerical scale. Journal of clinical pathology. 1988; 41:467–470. [PubMed: 3366935]
29. Silber R, Conklyn M, Grusky G, Zucker-Franklin D. Human lymphocytes: 5'-nucleotidase-positive and -negative subpopulations. J Clin Invest. 1975; 56:1324–1327. [PubMed: 1184753]
30. Pardo A, Gibson K, Cisneros J, Richards TJ, Yang Y, Becerril C, et al. Up-regulation and profibrotic role of osteopontin in human idiopathic pulmonary fibrosis. PLoS medicine. 2005; 2:e251. [PubMed: 16128620]
31. Khalil N, O'Connor RN, Unruh HW, Warren PW, Flanders KC, Kemp A, et al. Increased production and immunohistochemical localization of transforming growth factor-beta in idiopathic pulmonary fibrosis. American journal of respiratory cell and molecular biology. 1991; 5:155–162. [PubMed: 1892646]
32. Wang L, Fan J, Thompson LF, Zhang Y, Shin T, Curiel TJ, et al. CD73 has distinct roles in nonhematopoietic and hematopoietic cells to promote tumor growth in mice. J Clin Invest. 2011; 121:2371–2382. [PubMed: 21537079]
33. Peng Z, Fernandez P, Wilder T, Yee H, Chiriboga L, Chan ES, et al. Ecto-5'-nucleotidase (CD73) - mediated extracellular adenosine production plays a critical role in hepatic fibrosis. FASEB journal : official publication of the Federation of American Societies for Experimental Biology. 2008; 22:2263–2272. [PubMed: 18263696]
34. Fernandez P, Perez-Aso M, Smith G, Wilder T, Trzaska S, Chiriboga L, et al. Extracellular generation of adenosine by the ectonucleotidases CD39 and CD73 promotes dermal fibrosis. The American journal of pathology. 2013; 183:1740–1746. [PubMed: 24266925]
35. Karmouty-Quintana H, Zhong H, Acero L, Weng T, Melicoff E, West JD, et al. The A2B adenosine receptor modulates pulmonary hypertension associated with interstitial lung disease. FASEB journal : official publication of the Federation of American Societies for Experimental Biology. 2012; 26:2546–2557. [PubMed: 22415303]
36. Cronstein BN. Adenosine receptors and fibrosis: a translational review. F1000 biology reports. 2011; 3:21. [PubMed: 22003368]

37. Roberts VS, Cowan PJ, Alexander SI, Robson SC, Dwyer KM. The role of adenosine receptors A2A and A2B signaling in renal fibrosis. Kidney international. 2014; 86:685–692. [PubMed: 25054776]

38. Chunn JL, Mohsenin A, Young HW, Lee CG, Elias JA, Kellems RE, et al. Partially adenosine deaminase-deficient mice develop pulmonary fibrosis in association with adenosine elevations. American journal of physiology Lung cellular and molecular physiology. 2006; 290:L579–L587. [PubMed: 16258000]

39. Burnstock G, Vaughn B, Robson SC. Purinergic signalling in the liver in health and disease. Purinergic signalling. 2014; 10:51–70. [PubMed: 24271096]

40. Schneider DJ, Lindsay JC, Zhou Y, Molina JG, Blackburn MR. Adenosine and osteopontin contribute to the development of chronic obstructive pulmonary disease. FASEB journal : official publication of the Federation of American Societies for Experimental Biology. 2010; 24:70–80. [PubMed: 19720619]

41. Takahashi F, Takahashi K, Okazaki T, Maeda K, Ienaga H, Maeda M, et al. Role of osteopontin in the pathogenesis of bleomycin-induced pulmonary fibrosis. American journal of respiratory cell and molecular biology. 2001; 24:264–271. [PubMed: 11245625]

42. Berman JS, Serlin D, Li X, Whitley G, Hayes J, Rishikof DC, et al. Altered bleomycin-induced lung fibrosis in osteopontin-deficient mice. American journal of physiology Lung cellular and molecular physiology. 2004; 286:L1311–L1318. [PubMed: 14977630]

43. Wu M, Schneider DJ, Mayes MD, Assassi S, Arnett FC, Tan FK, et al. Osteopontin in systemic sclerosis and its role in dermal fibrosis. The Journal of investigative dermatology. 2012; 132:1605–1614. [PubMed: 22402440]

44. Wan YY, Flavell RA. 'Yin-Yang' functions of transforming growth factor-beta and T regulatory cells in immune regulation. Immunological reviews. 2007; 220:199–213. [PubMed: 17979848]

45. Regateiro FS, Howie D, Nolan KF, Agorogiannis EI, Greaves DR, Cobbold SP, et al. Generation of anti-inflammatory adenosine by leukocytes is regulated by TGF-beta. European journal of immunology. 2011; 41:2955–2965. [PubMed: 21770045]

46. Chan ES, Cronstein BN. Adenosine in fibrosis. Modern rheumatology / the Japan Rheumatism Association. 2010; 20:114–122. [PubMed: 19949965]

47. Sun CX, Young HW, Molina JG, Volmer JB, Schnermann J, Blackburn MR. A protective role for the A1 adenosine receptor in adenosine-dependent pulmonary injury. J Clin Invest. 2005; 115:35–43. [PubMed: 15630442]

48. Eckle T, Grenz A, Laucher S, Eltzschig HK. A2B adenosine receptor signaling attenuates acute lung injury by enhancing alveolar fluid clearance in mice. J Clin Invest. 2008; 118:3301–3315. [PubMed: 18787641]

49. Ehrentraut H, Clambey ET, McNamee EN, Brodsky KS, Ehrentraut SF, Poth JM, et al. CD73+ regulatory T cells contribute to adenosine-mediated resolution of acute lung injury. FASEB journal : official publication of the Federation of American Societies for Experimental Biology. 2013; 27:2207–2219. [PubMed: 23413361]

50. Morschl E, Molina JG, Volmer JB, Mohsenin A, Pero RS, Hong JS, et al. A3 adenosine receptor signaling influences pulmonary inflammation and fibrosis. American journal of respiratory cell and molecular biology. 2008; 39:697–705. [PubMed: 18587054]

51. Sitkovsky MV. T regulatory cells: hypoxia-adenosinergic suppression and re-direction of the immune response. Trends in immunology. 2009; 30:102–108. [PubMed: 19201652]

52. Stagg J, Divisekera U, Duret H, Sparwasser T, Teng MW, Darcy PK, et al. CD73-deficient mice have increased antitumor immunity and are resistant to experimental metastasis. Cancer research. 2011; 71:2892–2900. [PubMed: 21292811]

53. Mandapathil M, Szczepanski MJ, Szajnik M, Ren J, Lenzner DE, Jackson EK, et al. Increased ectonucleotidase expression and activity in regulatory T cells of patients with head and neck cancer. Clinical cancer research : an official journal of the American Association for Cancer Research. 2009; 15:6348–6357. [PubMed: 19825957]

54. Stagg J, Divisekera U, McLaughlin N, Sharkey J, Pommey S, Denoyer D, et al. Anti-CD73 antibody therapy inhibits breast tumor growth and metastasis. Proceedings of the National

Academy of Sciences of the United States of America. 2010; 107:1547–1552. [PubMed: 20080644]

55. Vermaelen K, Pauwels R. Accurate and simple discrimination of mouse pulmonary dendritic cell and macrophage populations by flow cytometry: methodology and new insights. Cytometry Part A : the journal of the International Society for Analytical Cytology. 2004; 61:170–177. [PubMed: 15382026]

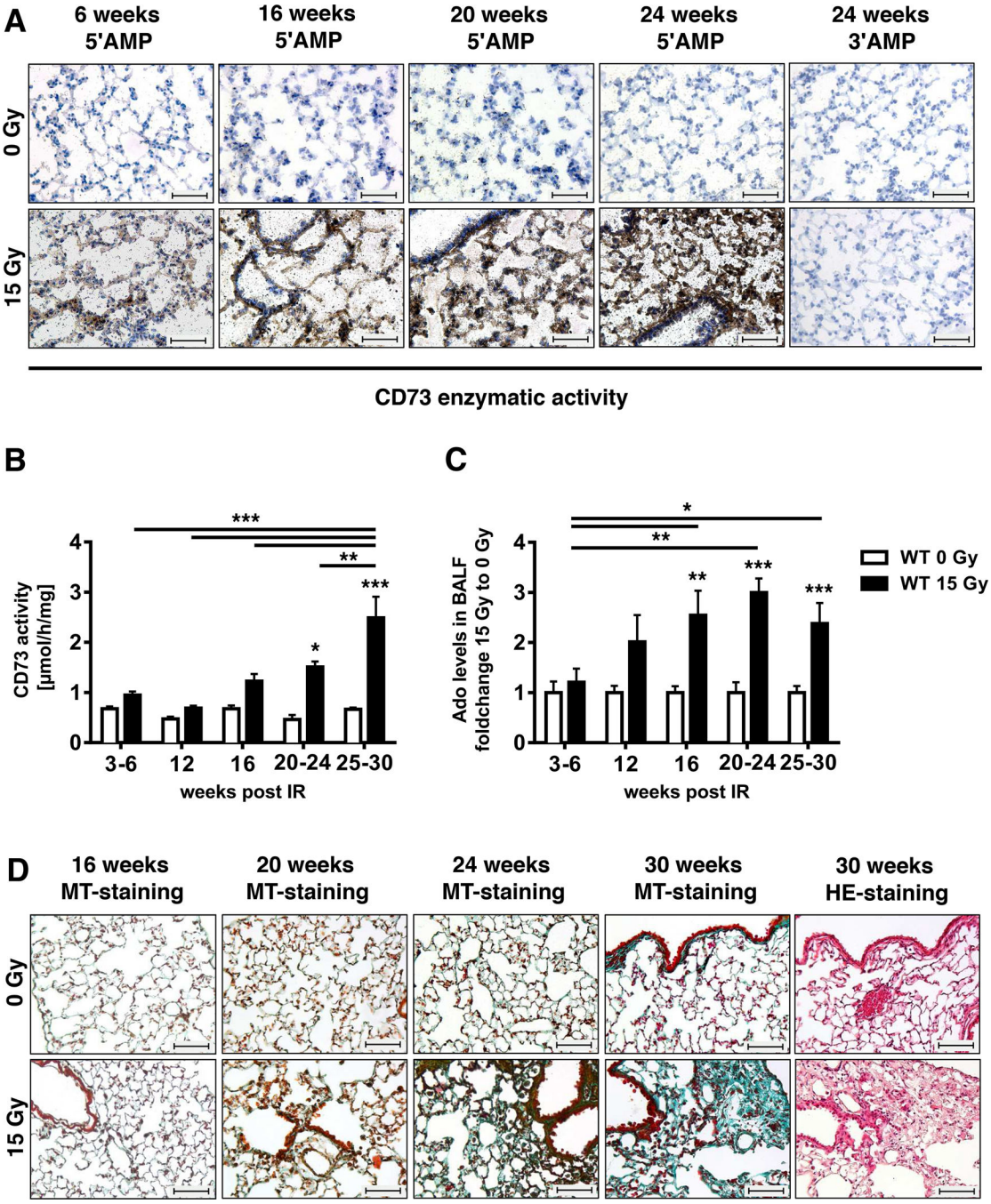

Figure 1. Radiation induces up-regulation of CD73, adenosine accumulation and lung fibrosis

C57BL/6 WT mice received 0 or 15 Gy WTI and were sacrificed at the indicated time points post-irradiation. (**A**) CD73 histochemistry on lung frozen sections of irradiated and control mice using 5'-AMP or 5'-AMP (negative control) as substrates. CD73 activity is visualized by the black lead sulfide precipitate. (**B**) Lung CD73 enzyme activity at the indicated time points (n = 12/12, 9/9, 10/9, 5/4, 19/13 [0 Gy/15 Gy]). (**C**) Fold change of BALF adenosine levels (mean ± SEM) of irradiated vs. control mice. Means of control values were between 41 and 149.5 nM (n = 9/10, 7/7, 10/9, 8/7, 20/11 [0 Gy/15 Gy]). *$P \leq 0.05$, **$P \leq 0.01$, ***P

≤ 0.001 by two-way ANOVA followed by post-hoc Bonferroni test. (**D**) Masson´s Goldner Trichrome (MT) and H&E staining of paraffin-embedded lung sections (scale bar = 100 μm).

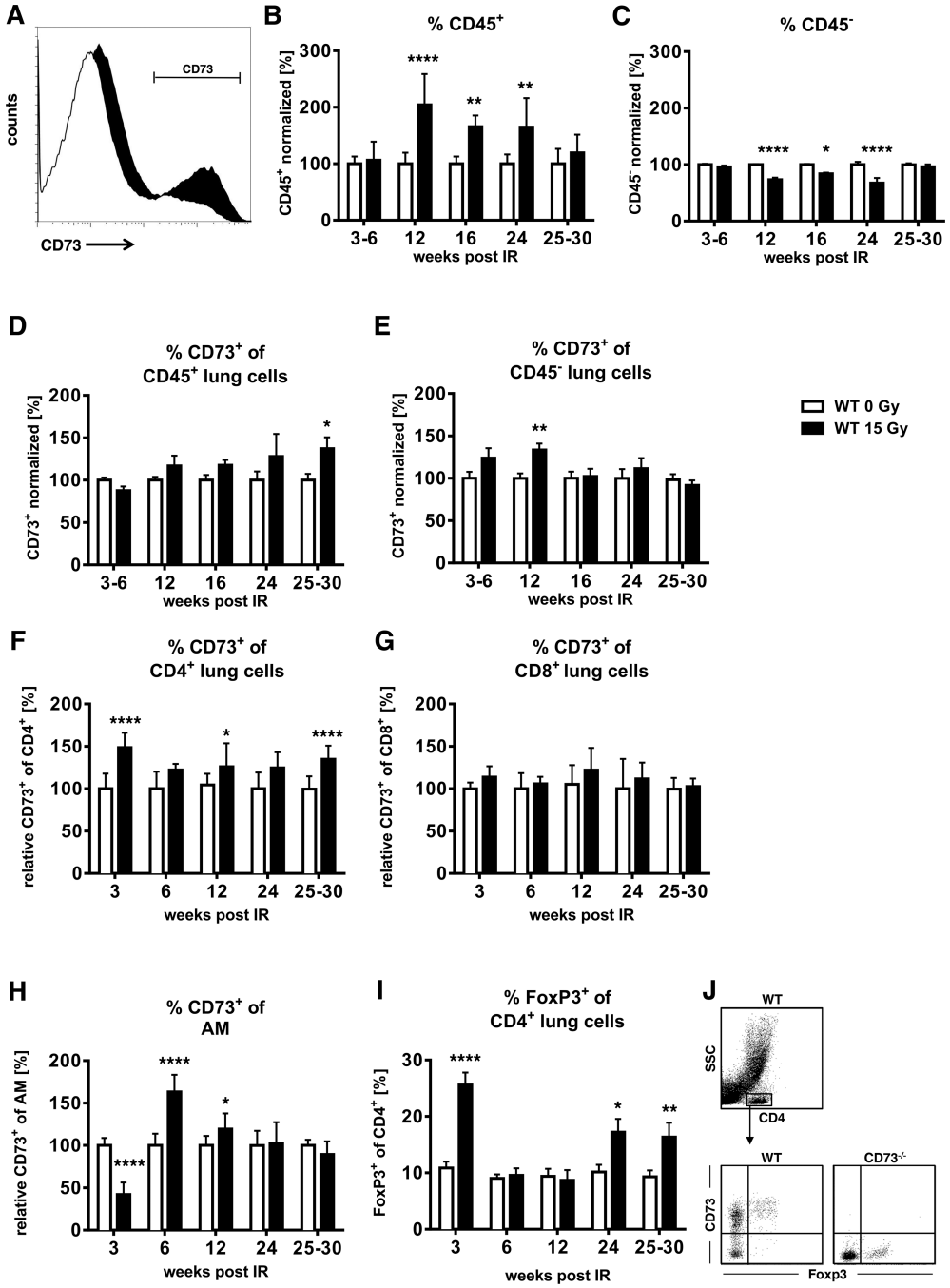

Figure 2. Thoracic irradiation triggers time-dependent alterations in CD73 expression on resident cells and immune cells

C57BL/6 WT mice received 0 or 15 Gy WTI and were sacrificed at the indicated time points post-irradiation. Whole lung cell (WLC) CD45 and/or CD73 expression were analyzed by flow cytometry. (**A**) CD73 expression in WLC is shown in the black histogram. (**B, C**) Normalized percentages of $CD45^+$ (**B**, n = 11/11, 16/16, 6/6, 6/5, 10/12) or CD45 (**C**, n = 15/11, 16/16, 6/6, 6/5, 10/12) WLC. (**D-H**) Normalized percentages of $CD45^+$, CD45, $CD4^+$, $CD8^+$ cells and alveolar macrophages ($CD11c^{hi}$ autofluorescent (55)) with CD73

surface expression (**D**, n = 11/11, 16/16, 6/6, 6/5, 10/12; **E**, n = 11/11, 16/16, 6/6, 6/5, 9/11**; F, G** n = 7/7, 7/7, 14/14, 6/6, 15/15; **H**, n = 10/10, 8/8, 12/12, 6/4, 6/4). (**I**) Percentages of lung $CD4^+$ regulatory T cells ($FoxP3^+$) (n = 7/6, 11/11, 9/9, 7/7, 13/8) (mean ± SEM . $*P \leq 0.05$, $**P \leq 0.01$, $****P \leq 0.0001$ by unpaired two-tailed t-test. (**J**) Gating strategy of $CD4^+$ cells for CD73 and $FoxP3^+$ expression evaluation.

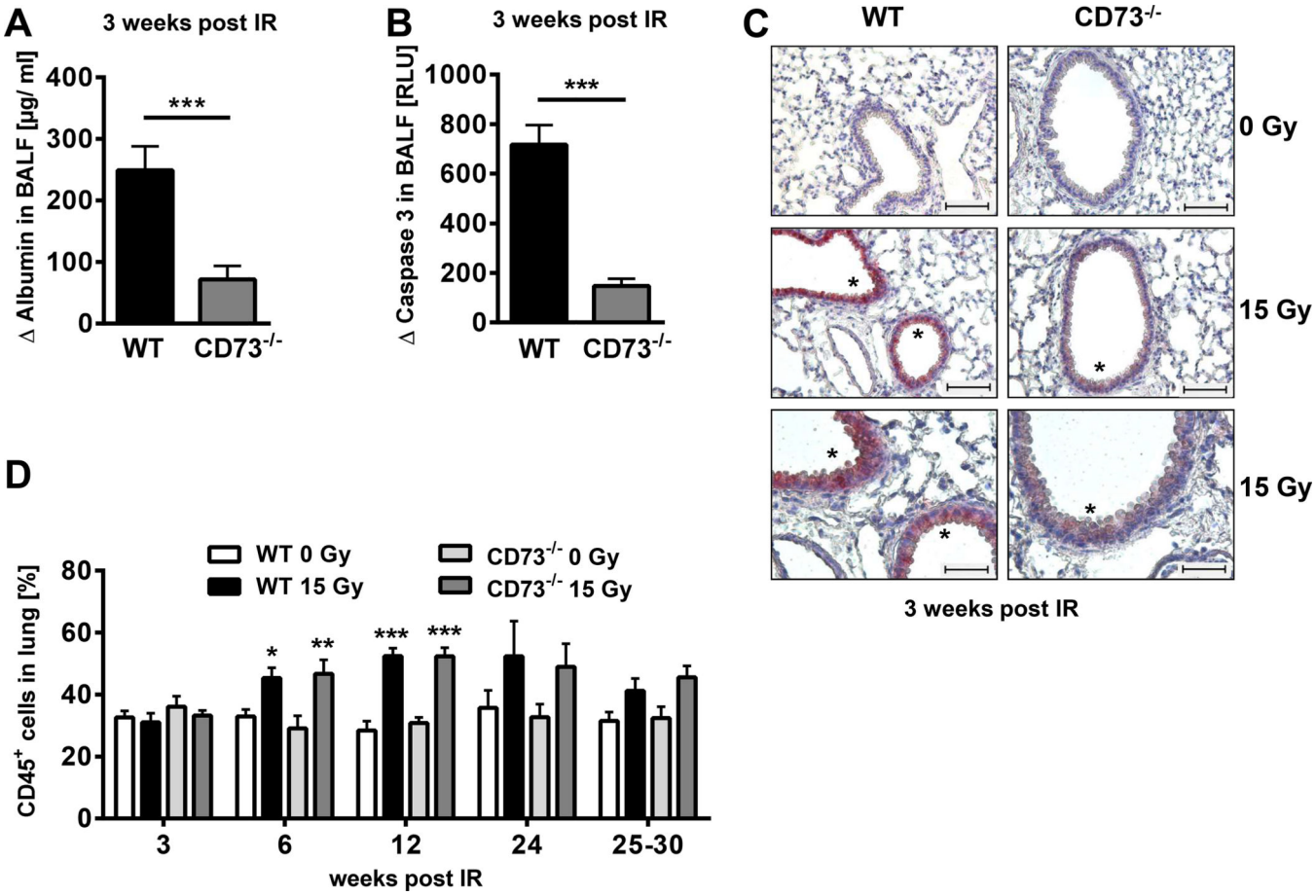

Figure 3. CD73$^{-/-}$ mice exhibit decreased early damage to resident cells but similar leukocyte recruitment in response to ionizing radiation

C57BL/6 WT and CD73$^{-/-}$ mice received 0 or 15 Gy hemithorax irradiation (A, B) or WTI (C, D). (**A**) Differences in BALF albumin levels of irradiated WT versus CD73$^{-/-}$ mice (Δ albumin) at 3 weeks post-irradiation by ELISA (n = 4/5). (**B**) Differences in BALF active caspase 3 of WT versus CD73$^{-/-}$ mice (Δ caspase 3) by luminescence [RLU] at 3 weeks post-irradiation (n = 3/3). (**C**) Active caspase 3 on paraffin-embedded lung sections (lower panels are a 2× enlargement of middle panels: upper & middle panels: scale bar = 100 µm; lower panels: scale bar = 50 µm). Asterisks depict regions with active caspase 3. (**D**) Time-course of radiation-induced infiltration of CD45^{+} cells (%) in WT and CD73$^{-/-}$ mice (n = 10/10/10/10, 10/10/10/10, 12/12/12/11, 6/4/6/5, 10/8/8/9 [WT 0 Gy/WT 15 Gy/CD73$^{-/-}$ 0 Gy/CD73$^{-/-}$ 15 Gy]. Data show means ± SD (**A, B**) or means ± SEM (**D**). *$P \leq 0.05$, **$P \leq 0.01$, ***$P \leq 0.001$ by unpaired two-tailed t-test (**A, B**) or two-way ANOVA followed by post-hoc Bonferroni test (**D**).

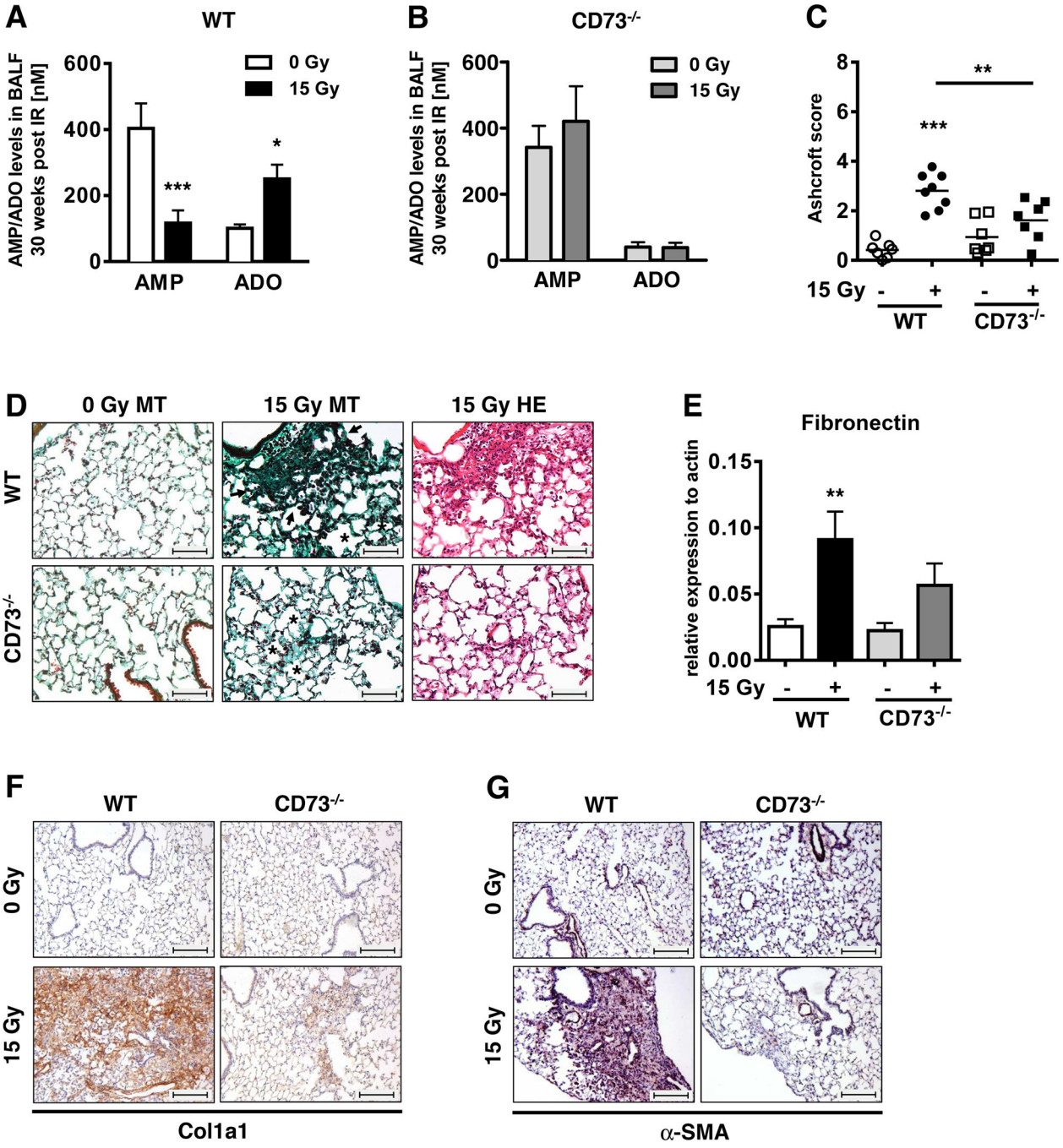

Figure 4. Genetic deficiency of CD73$^{-/-}$ prevents radiation-induced accumulation of adenosine and attenuates radiation-induced lung fibrosis

CD73$^{-/-}$ and WT mice received 0 or 15 Gy WTI and were sacrificed at ≥25 weeks post-irradiation. Adenosine and AMP levels in BALF for (**A**) C57BL/6 WT and (**B**) CD73$^{-/-}$ mice (mean ± SEM, n = 16/9, 23/14 (**A**); n = 7/4, 8/6 (**B**). (**C**) Quantification of fibrosis in WT (n = 7/8) and CD73$^{-/-}$ (n = 7/7) mice by Ashcroft scores; horizontal lines represent mean values. (**D**) MT and H&E stained lung sections. Asterisks emphasize thickening of alveolar wall structures and arrowheads fibrotic regions (scale bar = 100 μm). (**E**) qPCR

analysis of fibronectin expression normalized to actin (n = 9/10/7/8). Immunohistochemical stainings of paraffin-embedded lung sections for Collagen Type 1 (**F**) and α-SMA expression (**G**). Scale bar = 200 μm. Data show means ± SEM. $*P \leq 0.05$, $**P \leq 0.01$, $***P \leq 0.001$ by two-way ANOVA followed by post-hoc Bonferroni test (A, B), one-way ANOVA followed by post-hoc Newman-Keuls test (C, E) or representative pictures (D, F, G).

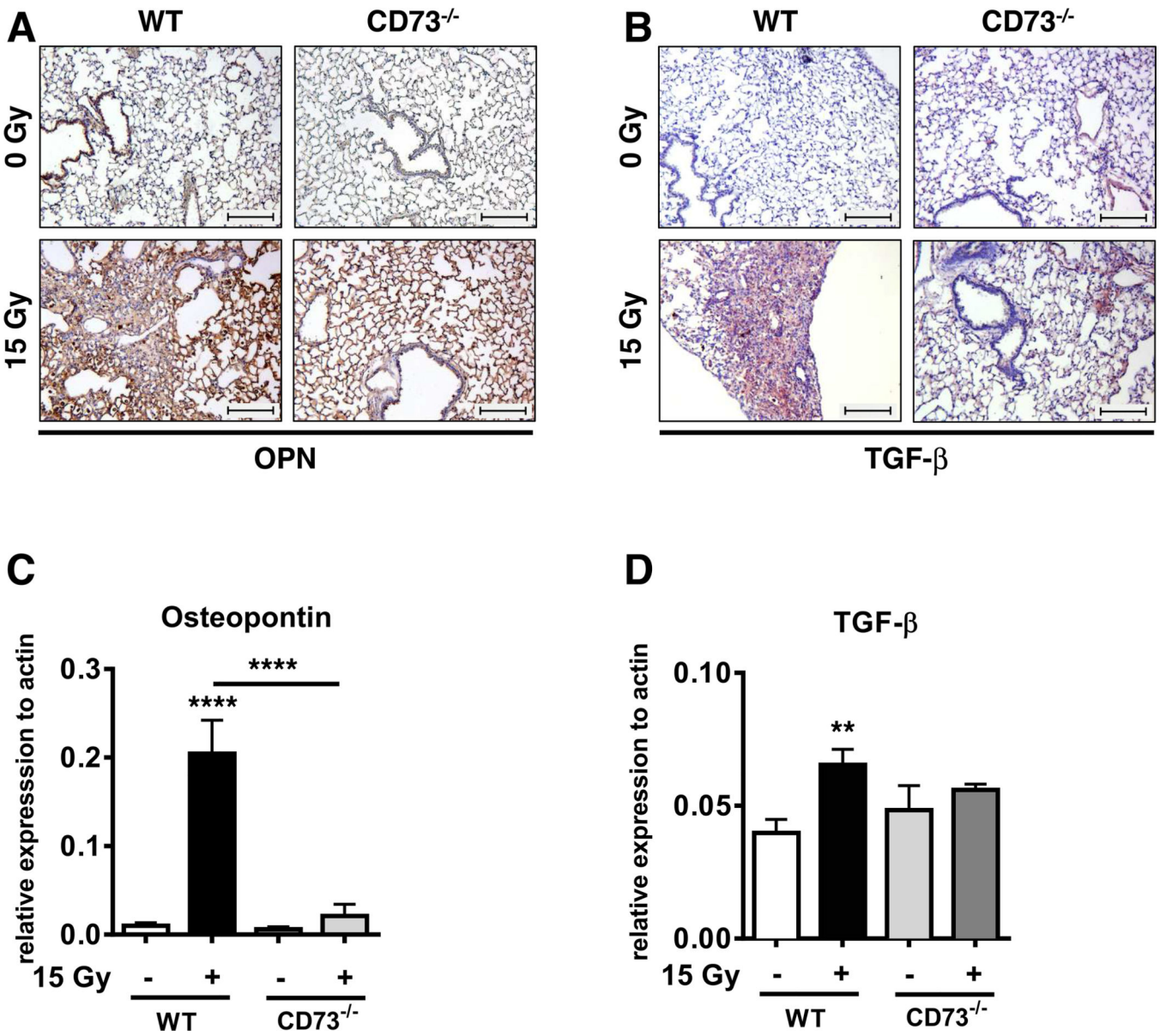

Figure 5. Genetic deficiency of CD73$^{-/-}$ prevents radiation-induced accumulation of the pro-fibrotic markers osteopontin and TGF-β

WT and CD73$^{-/-}$ mice received 0 or 15 Gy WTI and were sacrificed at ≥25 weeks post IR. (**A+B**) Immunohistochemical staining of paraffin-embedded lung sections for osteopontin (**A**) or TGF-β expression (**B**). Scale bar = 200 μm. qPCR analysis for (**C**) osteopontin (n = 7/7, 4/4) and (**D**) TGF-β (n = 14/11, 7/8) expression normalized to actin. Shown are means ± SD (CD73$^{-/-}$) or SEM (WT). $^{**}P \leq 0.01$, $^{****}P \leq 0.0001$ by one-way ANOVA followed by post-hoc Newman-Keuls test.

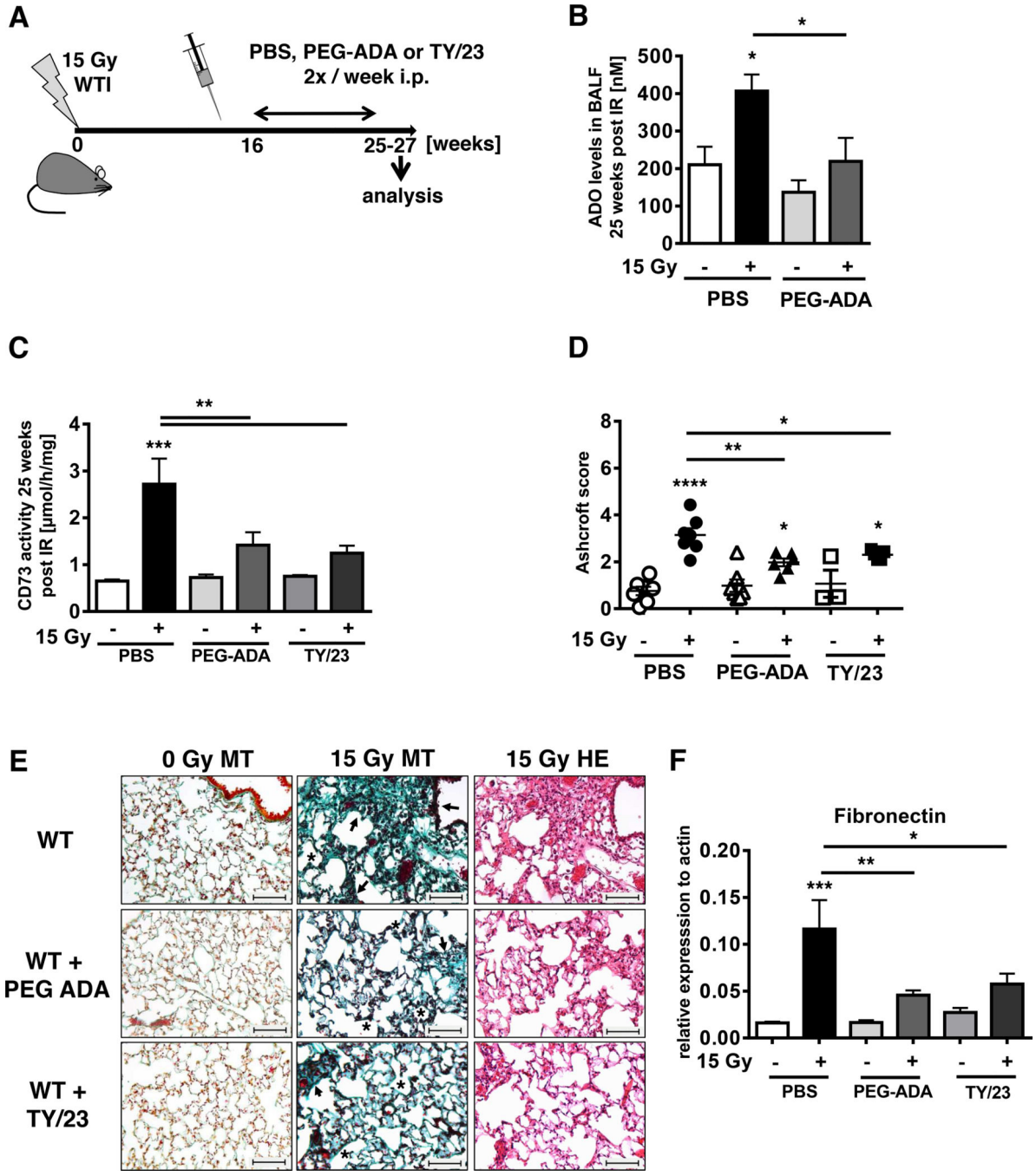

Figure 6. PEG-ADA or mAb TY/23 reduce radiation-induced lung fibrosis

C57BL/6 mice irradiated with 0 Gy or 15 Gy WTI were treated with PBS, PEG-ADA (5 units) or mAb TY/23 (100 µg) twice weekly i.p. beginning at week 16. (**A**) Schematic depiction of the experimental setup. (**B**) Adenosine levels [nM] in BALF from WT mice at 25 weeks post-irradiation ± treatment with PEG-ADA (n = 6/6, 5/6). (**C**) CD73 enzyme activity in lungs of WT mice 25 weeks post-irradiation ± treatment with PEG-ADA or TY/23 (n = 9/9, 8/9, 3/6). (**D**) Ashcroft scores of WT mice ± PEG-ADA or TY/23 at 25 weeks post-irradiation (n = 7/7, 7/6, 3/5). Horizontal lines represent means. (**E**) MT or H&E

stained lung sections from WT mice with PBS, PEG-ADA or TY/23 treatment at ≥ 25 weeks post irradiation. Asterisks emphasize thickening of alveolar wall structures and arrowheads fibrotic regions (scale bar = 100 μm). (**F**) qPCR analysis of fibronectin expression normalized to actin (n = 8/9, 7/9, 3/6) at ≥ 25 weeks post irradiation (mean ± SEM, **B-D, F**). $*P \leq 0.05$, $**P \leq 0.01$, $***P \leq 0.001$, $****P \leq 0.0001$ by one-way ANOVA followed by post-hoc Newman-Keuls test (**B, C, D, F**).